



Contents lists available at ScienceDirect



Catalysis Today

journal homepage: www.elsevier.com/locate/cattod

Effects of the precipitation agents and rare earth additives on the structure and catalytic performance in glycerol hydrogenolysis of Cu/SiO₂ catalysts prepared by precipitation-gel method

Zhiwei Huang ^{a,b}, Hailong Liu ^{a,c}, Fang Cui ^a, Jianliang Zuo ^a, Jing Chen ^{a,b,*}, Chungu Xia ^{a,b,*}

^a State Key Laboratory for Oxo Synthesis and Selective Oxidation, Lanzhou Institute of Chemical Physics, Chinese Academy of Sciences, Lanzhou 730000, China

^b Suzhou Institute of Nano-Tech and Nano-Bionics, Chinese Academy of Sciences, Suzhou 215123, China

^c University of Chinese Academy of Sciences, Beijing 100039, China

ARTICLE INFO

Article history:

Received 23 October 2013

Received in revised form 25 February 2014

Accepted 27 February 2014

Available online xxxx

Keywords:

Glycerol hydrogenolysis

1,2-Propanediol

Cu/SiO₂ catalyst

Precipitation agent

Rare earth additive

ABSTRACT

The effects of the precipitation agents (NaOH, Na₂CO₃, NH₄OH and NH₄HCO₃) and rare earth additives (La, Ce, Y, Pr and Sm) were studied on the structure and catalytic performance in glycerol hydrogenolysis of the Cu/SiO₂ catalysts prepared by precipitation-gel method. The physical-chemical properties of the catalysts were characterized by means of FTIR, H₂-TPR, N₂O chemisorption, XRD, XPS, BET and TEM. The results showed that precipitation agents had obvious effects on the phase structure, reduction property and catalytic performances (activity, selectivity and stability) of the catalysts. The Cu/SiO₂ catalyst precipitated with NaOH presented the highest activity and stability than those with other precipitants, most likely due to its more even dispersion of Cu particles, higher resistant to sintering during glycerol reaction. The incorporation of rare earth additives to Cu/SiO₂ catalyst could promote the structural stability and inhibit the sintering and leaching of the catalysts, especially noticeable for Y and La, and thus contribute to the long-term stability of the catalysts. Clearly, this study provides directions for the design of more efficient and stable Cu catalysts toward the industrial application of glycerol hydrogenolysis.

© 2014 Elsevier B.V. All rights reserved.

1. Introduction

The utilization of biomass for the production of renewable chemicals and fuels, which provides an alternative to petroleum-based products, is gaining attention over the past decades [1–4]. 1,2-Propanediol (1,2-PDO) is an important commodity chemical widely used as functional fluids such as antifreezes, coolants, and as precursors in the synthesis of polyester resins and pharmaceuticals, etc. Currently, 1,2-PDO is commercially produced by the multi-step transformation of petroleum-derived propylene via its epoxide intermediate. This process suffers from a number of disadvantages such as low energy efficiency, environmental pollution and high feedstock costs. Therefore, the use of cheap and renewable alternative feedstock, such as glycerol, for the production of 1,2-PDO,

has attracted many efforts [5–7]. Glycerol is a main byproduct in the biodiesel production process by transesterification of vegetable oils and animal fats, and the catalytic hydrogenolysis of glycerol to value-added 1,2-PDO can contribute to the economy of the whole process.

So far, several types of the catalysts reported for glycerol hydrogenolysis are supported noble metal catalysts (e.g. Ru, Rh and Pt) [8–12] and transition metal-based catalysts (e.g. Cu, Ni, Co) [7,13–21]. Although the noble metals exhibit good activity for glycerol hydrogenolysis, their disadvantages of high cost and poor selectivity to 1,2-PDO discourage their extensive applications. Due to its high efficiency for C–O bond hydro-dehydrogenation and poor activity for C–C bond cleavage, copper is a known favorable catalyst for the hydrogenolysis of glycerol to 1,2-PDO, and various supports including SiO₂ [14,21], ZnO [16,22], Al₂O₃ [15,23], ZrO₂ [24], MgO [25], Cr₂O₃ [13,26] as well as ZnO–Al₂O₃ [27], MgAlO_x [19] and zeolite [15,28] have been explored for the preparation of efficient Cu-based catalysts (Table 1). Glycerol with conversions from 11 to 100% and 1,2-PDO selectivities from 83.9 to 100% were generally obtained over these Cu catalysts depending on the catalysts and reaction conditions (Table 1).

* Corresponding authors at: State Key Laboratory for Oxo Synthesis and Selective Oxidation, Lanzhou Institute of Chemical Physics, Chinese Academy of Sciences, Lanzhou 730000, China. Tel.: +86 931 4968089; fax: +86 931 4968129.

E-mail addresses: chenj@lzb.ac.cn (J. Chen), cgxia@lzb.ac.cn (C. Xia).

Table 1

Typical Cu catalysts and their catalytic performances in glycerol hydrogenolysis to 1,2-propanediol since 2007.

Catalyst (mass or volume)	Reactant and reactor	Reaction conditions	Conv. (%)	Sel. (%)	Ref.
Cu/ZnO (2.2 g)	50 mL 20 wt%Gly ^b , ABR ^c	473 K, 6 MPa, 6 h	75	94	[16]
CuO/ZnO-OG ^a (3 g)	140 mL pure Gly, ABR	473 K, 5 MPa, 7 h	46	90	[22]
Cu-Ga ₂ O ₃ /ZnO (2.8 g)	177 g, 90 wt%Gly, ABR	493 K, 5 MPa, 7 h	96	82	[29]
Cu/Al ₂ O ₃ (2.7 mmol)	65 g 50 wt% Gly, ABR	493 K, 1.5 MPa, 10 h	49.6	96.8	[15]
Cu-Ag/Al ₂ O ₃ (~1 g)	65 g 50 wt% Gly, ABR	473 K, 1.5 MPa, 10 h	27	96	[23]
Cu/ZnO/Al ₂ O ₃	pure Gly, WHSV ^e =0.08 h ⁻¹ , FBR ^d	463 K, 0.64 MPa	96.2	92.2	[27]
Cu/ZrO ₂ (0.6 g)	25 g 20 wt%Gly, ABR	473 K, 4.0 MPa, 8 h	11	90	[24]
Cu/MgO (1.0 g)	8 mL 75 wt%Gly, ABR	453 K, 3 MPa, 20 h	72.0	97.6	[25]
Cu _{0.4} /Zn _{0.6} Mg _{5.0} Al ₂ O _{8.6} (0.4 g)	8 g 75 wt%Gly, ABR	473 K, 2 MPa, 10 h	85.5	98.6	[19]
Cu/SiO ₂ (4 g)	40 wt% Gly, WHSV=0.25 h ⁻¹ , FBR	453 K, 6.0 MPa	80	98	[14]
Cu-B/SiO ₂ (4 g)	10 wt% Gly, LHSV ^f =0.075 h ⁻¹ , FBR	473 K, 5 MPa	100	98.0	[21]
Cu/SBA-15 (0.35 g)	120 mL 40 V%Gly, ABR	513 K, 8 MPa, 5 h	52.0	96.2	[28]
Cu-H ₄ SiW ₁₂ O ₄₀ /Al ₂ O ₃ (5 g)	10 wt% Gly, LHSV=0.9 h ⁻¹ , FBR	513 K, 6 MPa	90.1	89.7	[30]
Cu-Cr (1 g)	50 g 90 wt%Gly, ABR	493 K, 8 MPa, 12 h	80.3	83.9	[31]
Cu-Cr (0.009 mol)	18 g pure Gly, ABR	403 K, 2 MPa, 4 h	22.2	100	[26]
Cu-Cr-Ba (23 g)	30 mL/h 20 wt%Gly, FBR	493 K, 4 MPa	65	>91	[32]

^a OG: prepared by an oxalate gel method.^b Gly=glycerol.^c ABR: autoclave batch reactor.^d FBR: fixed-bed reactor.^e WHSV: weight hourly space velocity.^f LHSV: liquid hourly space velocity.

Due to their excellent selectivity, green benefit, and low cost, Cu/SiO₂ catalysts have attracted considerable attention in glycerol hydrogenolysis to 1,2-PDO [14,21,28,33–35]. Previously, we reported that the Cu/SiO₂ catalyst with high dispersion prepared by precipitation-gel (PG) method exhibited high efficiency and good stability in the hydrogenolysis of glycerol to 1,2-PDO [14]. Nevertheless, the single-component Cu/SiO₂ catalyst still encounters some technical problems, such as insufficient catalytic activity and stability for glycerol hydrogenolysis. To address these problems requires the development of improved catalysts, which could be achieved by improving the preparation technique and incorporating of proper promoters [14,21,28,29,36]. For example, the incorporation of B [21], Ga [29] and La [36] has been reported to be effective for stabilizing the active Cu species in glycerol hydrogenolysis.

It is well known that the structure and catalytic performances of the Cu catalysts prepared by precipitation significantly affected by the precipitation agents. For example, Dong et al. [37] found that the activities of CuO–CeO₂–ZrO₂ catalysts in CO oxidation prepared with different precipitants decreased in the order of Na₂CO₃ > NH₄OH > (NH₄)₂CO₃ > NaOH, and ascribed the best performance of the catalyst prepared by Na₂CO₃ to smaller grains with uniform distribution. The composition of the precipitants was also found to affect the structure and catalytic performances of the Cu catalysts, e.g. the residual sodium in the Cu/SiO₂ catalyst prepared by PG method using NaOH as precipitant profoundly affected the physicochemical properties and catalytic performance of the catalyst in glycerol hydrogenolysis [33]. Thus, the detailed comparative study regarding the influence of precipitation agent on the physicochemical properties of the Cu/SiO₂ catalysts prepared by PG method and their catalytic performance in glycerol hydrogenolysis would be helpful for the understanding of the key fundamental issues including the effect of catalyst structures and functions. In the present work, four different precipitants, i.e. NaOH, Na₂CO₃, NH₄OH and NH₄HCO₃, were used to study the effects of the precipitation agents on the structures and catalytic performances in glycerol hydrogenolysis of the Cu/SiO₂ catalysts prepared by PG method. A variety of rare earth (RE) elements including La, Ce, Y, Pr and Sm were incorporated into the Cu/SiO₂ catalyst prepared by PG method in order to reveal the promotion effect of the rare earth additives and further improve the reaction stability of the catalyst.

2. Experimental

2.1. Catalyst preparation

The CuO/SiO₂ catalyst precursor prepared by PG method with NaOH is as follows: first, an aqueous solution of NaOH (15 wt%) was dropped into a solution of Cu(NO₃)₂ (0.5 mol/L) at a constant rate under vigorous stirring to form precipitate till pH >11. Next, a calculated amount of colloidal aqueous silica solution (SiO₂, 40.0 wt%, Guangzhou Renmin Chemical Plant, China) was added to the solution of the precipitate to form a gel, and then the gel was allowed to age at around 353 K for 4 h. Finally, the slurry of the gel was filtered, thoroughly washed with hot distilled water, dried at 393 K overnight, and calcined at 723 K under air for 3 h. The procedures for the preparation of Cu/SiO₂ catalysts with Na₂CO₃, NH₄HCO₃ and NH₄OH are similar to that for NaOH with the same precipitant concentration while the pH of the precipitate for NH₄HCO₃ and NH₄OH is around 7. The normal Cu loading of the samples was 25.5 wt%, and the dried and calcined samples were denoted as PGO-base, while the reduced active catalyst was named as PG-base, e.g. the calcined sample and reduced catalyst prepared with NaOH are as PGO-NaOH and PG-NaOH, respectively.

The RE-incorporated CuO/SiO₂ precursors were prepared as follows: preparation the mother CuO/SiO₂ sample by PG method with NaOH as mentioned above, then impregnation the mother CuO/SiO₂ sample with an aqueous solution of RE(NO₃)_x (RE = La, Ce, Y, Pr and Sm) to obtain the required final REO_x loading. The sample was dried under the same conditions as the catalyst prepared by PG method, and calcined at 723 and 1023 K for 3 h to obtain the final CuO–REO_x–SiO₂ samples. The compositions and codes of the CuO–REO_x–SiO₂ samples are listed in Table 5.

2.2. Catalyst characterization

Fourier transform infrared (FTIR) spectra were recorded at room temperature on powdered samples using the KBr wafer technique in a Nicolet Nexus 870 FTIR spectrometer. The X-ray powder diffractions (XRD) of the samples were obtained on a PANalytical X'pert Pro Diffractometer using nickel filtered Cu K α radiation (λ = 1.5418 Å) operated at 40 kV voltage and 30 mA. The average crystallite size of CuO was estimated from the average values at CuO(–1 1 1) (2θ = 35.5°) and (1 1 1) (2θ = 38.8°), and the average

crystallite size of Cu⁰ from the value at Cu(111) ($2\theta = 43.3^\circ$). X-ray photoelectron spectra (XPS) were obtained using a VG ESCALAB 210 spectrometer equipped with a Mg K α X-ray radiation source ($h\nu = 1253.6$ eV) and a hemispherical electron analyzer. All binding energies were calibrated using the Si2p peak at 103.4 eV as the reference.

Temperature-programmed reduction (TPR) measurements were carried out in a quartz U-tube reactor with 20 mg of sample used for each measurement. The samples were first pretreated at 473 K under He flow for 1 h and then reduced with 5% H₂/N₂ at a flow rate of 40 mL/min and the temperature was increased from 303 to 773 K at a ramping rate of 10 K/min. H₂ consumption was continuously monitored by a thermal conductivity detector (TCD).

The dispersions of the catalysts were determined by dissociative N₂O adsorption-H₂ temperature-programmed reduction (TPR) reverse titration experiments [16,38]. The catalysts were first reduced at 723 K with 5% H₂/N₂ at a flow rate of 40 mL/min for 1 h. After cooling to 323 K in a He flow, the reduced samples were exposed to a 5% N₂O/N₂ mixture (40 mL/min) for 40 min. Finally, the samples were cooled to room temperature to start another TPR run with 5% H₂/N₂ at a flow rate of 40 mL/min and a ramping rate of 10 K/min to 573 K. The copper metallic surface area, average copper particle size and dispersion were calculated by assuming 1.46×10^{19} copper atoms per m² and a molar stoichiometry N₂O/Cu_s = 0.5, where the symbol Cu_s means the copper atoms on the surface.

The BET surface area measurements were performed on a Micromeritics ASAP 2010 instrument at liquid nitrogen temperature. Prior to measurements, the samples were degassed at 573 K for 4 h. Transmission electron microscopic (TEM) investigations were carried out using a JEM2010 electron microscope at 200 kV.

2.3. Catalytic activity testing

The discontinuous glycerol reaction was carried out in a 200 mL stainless steel autoclave at a stirring speed of 400 rpm. Prior to the reaction, the CuO/SiO₂ samples were reduced at 553 K with a flowing 20%H₂/N₂ for 3 h. The standard reaction was carried out under the following reaction conditions: 6.4 MPa of initial H₂ pressure, 80 g of 80 wt% glycerol aqueous solution, 4 g of reduced catalyst, 12 h. After being purged, the reactor was heated to 453 K, and the reaction pressure was increased to about 9.0 MPa and maintained during the reaction. The liquid phase products were analyzed by using a gas chromatograph with a SE-54 capillary column (50 m × 0.32 mm) and a flame ionization detector. The gas products were analyzed by using a gas chromatograph (Porapak Q column (4 m × 3 mm)) equipped with a TCD. Products were also identified on a HP 6890/5793 GC-MS with a DB-5MS column. The detected products were 1,2-PDO, 1,3-PDO (trace), acetol, 1-propanol, 2-propanol (hydrogenolysis products); ethylene glycol (EG), ethanol, methanol, CH₄ and CO₂ (the degradation products). The glycerol conversion and selectivity to the reaction products were calculated on a carbon basis.

The continuous glycerol reaction was preformed in a vertical fixed-bed reactor at 6.0 MPa total pressure, employing 3–4 g of catalyst (20–40 mesh). The reactor tube was 36 cm long and 1.2 cm in inner diameter. The reactor was packed with the catalyst between two plugs of glass wool. Before the reaction, the catalysts were reduced with a hydrogen flow under atmospheric pressure at 553 K for 3 h. To increase the fluidity of the reaction media, 40 wt% glycerol in 10 wt% water and 50 wt% methanol were used. The solution was continuously pumped into the reactor with a high-pressure pump and preheated to around 373 K before transported into the reactor. Standard reaction conditions were: weight hourly space velocity (WHSV, of 0.25 g of glycerol solution per gram of catalyst

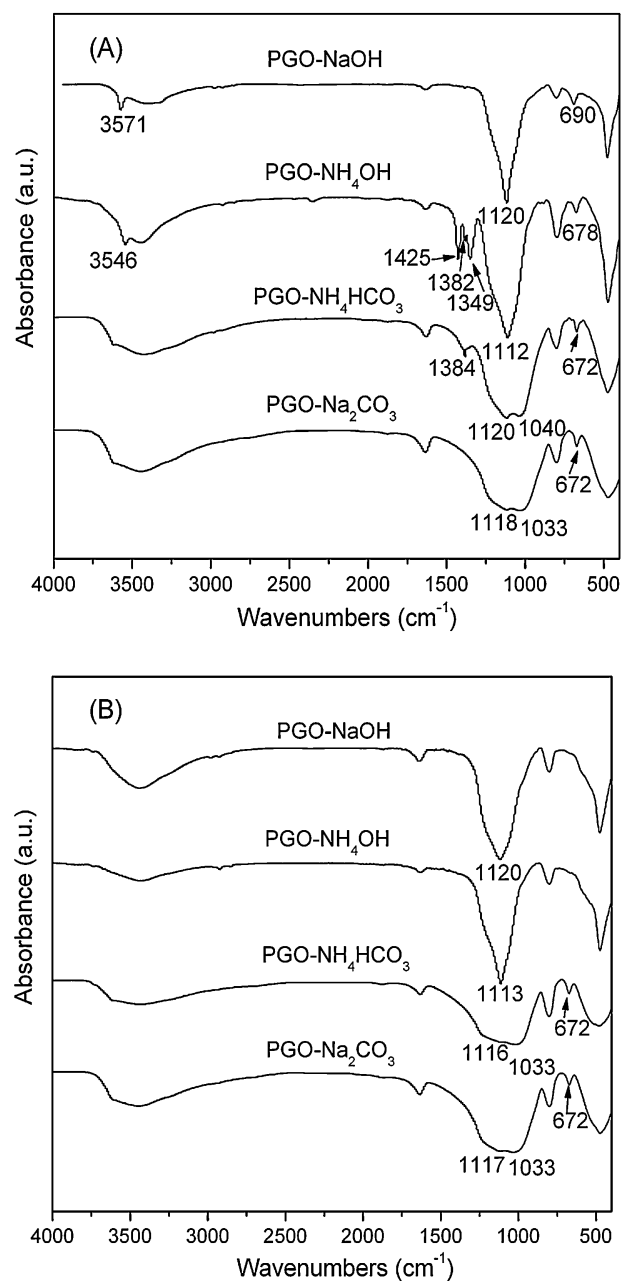


Fig. 1. FTIR spectra of dried (A) and calcined (B) samples prepared by different precipitation agents.

per hour) of 0.25 h⁻¹, glycerol to hydrogen ratio 1:23, 453 K. The reaction products were collected in an ice water bath and then analyzed as indicated above with ignoring the small amount of methanol generated during the reaction.

3. Results and discussion

3.1. Influence of the precipitation agents on the structure and catalytic performance of Cu/SiO₂ catalysts

FTIR experiments were carried out to study the structure and composition of the dried and calcined samples prepared with different precipitation agents. For dried PGO-Na₂CO₃ precursor (Fig. 1A), the apparent absorption bands at approximately 1120, 800, and 476 cm⁻¹ are assigned to the different vibration modes of

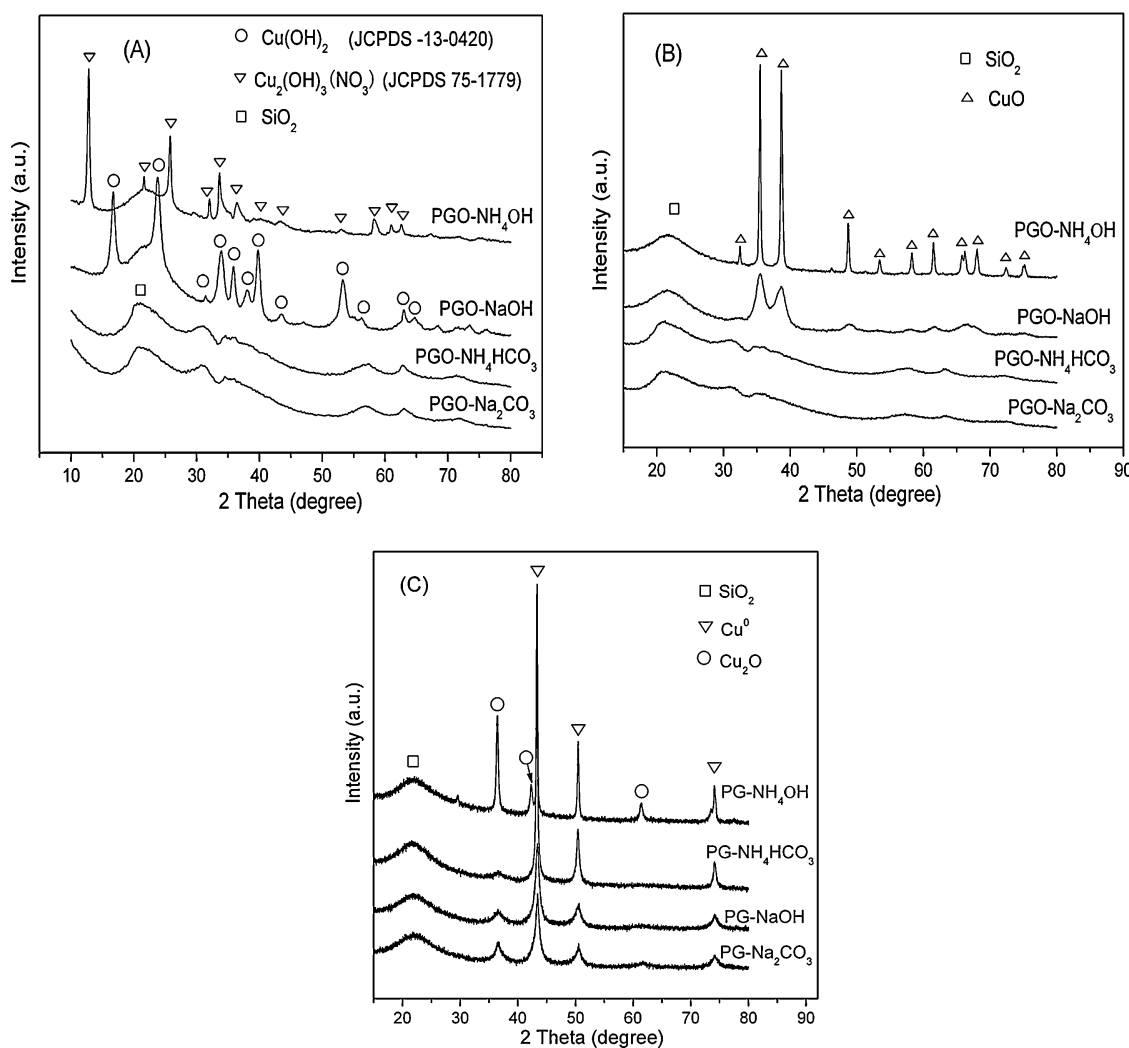


Fig. 2. XRD profiles of dried (A), calcined (B) samples and used catalysts (C) prepared by different precipitation agents.

the Si–O bonds in the amorphous SiO₂ [39,40]. The obvious peak at around 1033 cm⁻¹ on the low-frequency side of the ν_{SiO} band at 1120 cm⁻¹ together with the presence of the weak δ_{OH} band at around 672 cm⁻¹ indicates the presence of copper phyllosilicate [39]. The broad absorption band in the range 3200–3600 cm⁻¹ is due to the overlapping of the OH stretching vibration of adsorbed water and silanols [41]. In comparison with the dried PGO-Na₂CO₃ precursor, an additional small absorption at 1384 cm⁻¹ related to NO₃ groups is also observed in the profile of the dried PGO-NH₄HCO₃ precursor, suggesting the presence of a small amount of Cu₂(OH)₃NO₃ [39], beside copper phyllosilicate. The δ_{OH} band of the dried PGO-NaOH precursor appears at 690 cm⁻¹, revealing the presence of Cu(OH)₂ [39]. In the case of the dried PGO-NH₄OH precursor, the δ_{OH} band at 682 cm⁻¹ and sharp absorptions at 1349, 1382 and 1425 cm⁻¹ related to NO₃ groups are characteristic of the presence Cu₂(OH)₃NO₃ [39]. The hardly observation of the characteristic δ_{OH} band at around 672 cm⁻¹ and the ν_{SiO} band at around 1035 cm⁻¹ in the dried PGO-NaOH and PGO-NH₄OH precursors indicates that the copper phyllosilicate species formed in these two samples would be quite low.

After calcination at 723 K, the absorption bands associated with NO₃ groups in the dried PGO-NH₄OH and PGO-NH₄HCO₃ precursors and the characteristic δ_{OH} band of Cu(OH)₂ in the dried PGO-NaOH disappeared (Fig. 1B), suggesting the complete decomposition of Cu₂(OH)₃NO₃ and Cu(OH)₂ species to CuO after

calcination. The formation of CuO in calcined PGO-NH₄OH and PGO-NaOH sample is also confirmed by the XRD pattern given below. In contrast, no big difference was seen for both the ν_{SiO} band at around 1035 cm⁻¹ and the δ_{OH} band at around 672 cm⁻¹ for PGO-NH₄HCO₃ and PGO-Na₂CO₃ samples, referring that the structure of copper phyllosilicate in these samples was largely preserved, which is in line with the high stability of copper phyllosilicate reported previously [42].

The XRD profiles of the dried and calcined samples prepared by different precipitation agents are shown in Fig. 2A and B. The diffraction pattern of the sample precipitated by NaOH reveals the formation of a dispersed Cu(OH)₂ phase, while only sharp diffractions of Cu₂(OH)₃(NO₃) were detected in the sample prepared with NH₄OH. The apparent feature of dried samples precipitated with Na₂CO₃, NH₄HCO₃ was the broad and diffused diffraction of amorphous silica at around $2\theta = 22^\circ$. In addition, the weak and diffuse diffraction peaks at ca. 31.2° and 35.8° suggest the presence of copper phyllosilicate with poor crystallinity [39,43]. After calcination at 723 K, copper species in dried precursors of PGO-NaOH and PGO-NH₄OH were both converted to CuO (Fig. 2B). The diffraction peaks of CuO for the calcined PGO-NaOH sample are much broader and less intense than those of the PGO-NH₄OH sample, suggesting the former sample shows much smaller crystallite size (5.7 vs. 29.3 nm) and higher metal dispersion than those of the latter sample. Differently, no obvious difference was seen for the samples

precipitated with Na_2CO_3 and NH_4HCO_3 after calcination, suggesting the high stability of the copper species in these two samples, which is in line with the FTIR results.

Fig. 2C shows the XRD profiles of the catalysts after 12 h glycerol reaction at 453 K. Sharp and intensified diffraction peaks of metallic copper were seen in all used catalysts, with those for the used PG-NH₄OH and PG-NH₄HCO₃ much sharper. These findings suggest that copper species in PG-NH₄OH and PG-NH₄HCO₃ catalysts were seriously aggregated to much larger particles (40.2 nm and 26.4 nm, respectively) during glycerol reaction as compared to PG-Na₂CO₃ and PG-NaOH catalysts, which are 9.7 nm and 10.2 nm, respectively (**Table 2**), showing the much higher stability of the catalysts prepared by Na⁺ containing bases, probably due to that the residual Na⁺ in the catalyst could help retard the leaching of the active copper and reduce the aggregation of copper particles [33]. In addition, Cu₂O with different diffraction intensity is also observed in all used catalysts, which may be formed by the aggregation of the highly dispersed Cu₂O in the inadequately prereduced catalysts during glycerol reaction [14,35].

Table 2 shows the textural properties of the calcined CuO/SiO₂ samples prepared with different precipitation agents. The catalysts prepared with Na₂CO₃ and NH₄HCO₃ presented high surface areas of 345.1 and 382.6 m²/g, respectively, which are much higher than those of the catalysts prepared with NaOH (186.1 m²/g) and NH₄OH (112.5 m²/g). The larger surface areas of the catalysts prepared with NH₄HCO₃ and Na₂CO₃ would be ascribed to their higher dispersions, as which decreased in the order PG-NH₄HCO₃ > PG-Na₂CO₃ > PG-NaOH > PG-NH₄OH (**Table 2**), which is good consistent with the dispersion of the samples revealed by XRD. Additionally, the presence of larger amounts of copper phyllosilicate in the calcined PGO-NH₄HCO₃ and PGO-Na₂CO₃, as evidenced by FTIR, may also contribute to the higher surface areas of these samples [44]. The average pore diameters for these samples varied in a narrow range of 6.7–13.0 nm. As a result of Cu dispersion, the PG-NH₄HCO₃ and PG-Na₂CO₃ catalysts possessed relatively small Cu particle sizes of 3.3 and 3.8 nm, respectively, in comparison to 5.1 and 6.8 nm for PG-NaOH and PG-NH₄OH, respectively.

XPS experiments were carried out to determine the oxidation state of copper as well as the chemical compositions of the samples. The XP spectra of the calcined PGO-Na₂CO₃ and PGO-NH₄HCO₃ samples each showed a sharp photoelectron peak at around 936.2 eV (Cu2p_{3/2}), while the calcined PGO-NaOH and PGO-NH₄OH samples showed broad photoelectron peaks at about 935.5 eV with PGO-NH₄OH a bit lower, which is 935.3 eV (**Fig. 3** and **Table 3**). These high binding energy (BE) values along with the presence of the characteristic shakeup satellite peaks suggest that the copper oxidation state is +2 in all samples [45]. In comparison with the Cu2p_{3/2} BE of pure CuO, which was determined at 934.1 eV, such large positive BE shift of the Cu2p core level for these samples indicates the presence of copper phyllosilicate, according to our previous studies [35,46] and also references [43,44]. The presence of copper phyllosilicate in PGO-Na₂CO₃ and PGO-NH₄HCO₃ has been confirmed by FTIR analysis, as reported above (**Fig. 1**). The FWHM of the Cu2p_{3/2} spectra for PGO-NaOH and PGO-NH₄OH samples is above 4.1 eV, while that for PGO-Na₂CO₃ and PGO-NH₄HCO₃ samples is below 3.2 eV (**Table 3**). Such high FWHM of the Cu2p_{3/2} spectra for PGO-NaOH and PGO-NH₄OH infers the presence of two kinds of Cu(II) species, i.e. copper phyllosilicate and CuO (from XRD characterizations) in these samples. The Cu/Si ratio on the calcined PGO sample obtained by XPS analysis is 0.405, which is close to the bulk ratio (0.349) of the sample, suggesting a uniform dispersion of Cu species in the sample. The XPS surface Cu/Si atom ratios for PGO-Na₂CO₃ and PGO-NH₄HCO₃ samples are 4.0 and 3.5 times higher than their corresponding bulk ratios, respectively, revealing that copper species in both samples are largely enriched on the surface [47]. Differently, a much lower surface Cu/Si ratio (0.133)

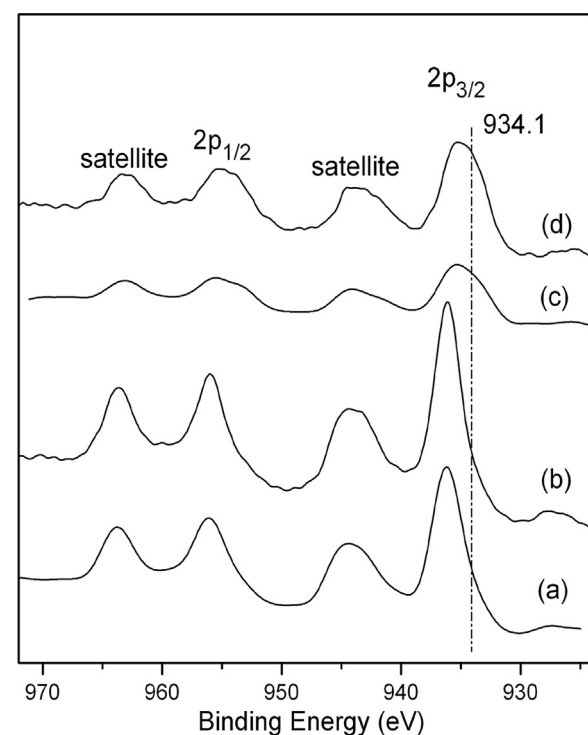


Fig. 3. XP spectra of the calcined CuO/SiO₂ samples prepared by different precipitation agents: (a) PGO-Na₂CO₃, (b) PGO-NH₄HCO₃, (c) PGO-NH₄OH and (d) PGO-NaOH.

is seen for calcined PGO-NH₄OH sample as compared to its bulk ratio (0.334), indicating serious aggregation of the sample [14,48], which supported the finding by XRD characterization. It is noteworthy that there was almost no detection of Na on the surface of PGO-NH₄HCO₃ and PGO-NH₄OH samples, which is in line with the AAS results compiled in **Table 2**.

Fig. 4 shows the TPR profiles of the CuO/SiO₂ samples prepared by different precipitation agents along with the reference of unsupported bulk CuO (from Alfa Aesar). As can be seen, PGO-NH₄OH sample showed a main reduction peak centered at 543 K and a small shoulder peak centered at a low temperature of 510 K. PGO-NH₄HCO₃ sample is reduced with a main reduction peak centered at 517 K and a weak shoulder peak centered around 533 K. Similar to PGO-NH₄HCO₃, PGO-Na₂CO₃ also showed two reduction peaks with the main peak present at 517 K and the obvious shoulder peak at 538 K. Differently, PGO-NaOH samples showed an unsymmetric hydrogen consumption peak centered around 534 K, while the unsupported pure CuO showed a good symmetric reduction peak centered around 549 K, which is around 6–16 K higher than that of the higher temperature peak of the CuO/SiO₂ samples.

Since dispersed CuO with small particle sizes can be more readily reduced to Cu⁰ than did the bulk CuO with larger sizes [45,49], while dispersed and surface interacted Cu²⁺ species are reported to be more difficult to be reduced to Cu⁰ than bulk CuO [50,51], because the further reduction of Cu⁺–Cu⁰ requires a much higher temperature (i.e. >873 K) [43]. Therefore, the reduction peak at 517 K or below for the CuO/SiO₂ samples prepared by NH₄OH, NH₄HCO₃ and Na₂CO₃ might be associated with the partial reduction of the highly dispersed surface interacted Cu²⁺ species, that is copper phyllosilicate, to Cu⁺. The presence of copper phyllosilicate in these samples has been verified by XPS characterization. The shoulder peaks in the high temperature range in these samples, which are close to that of the reduction of bulk CuO, could be ascribed to the reduction of separate CuO particles in these samples. For calcined PGO-NaOH sample, the unsymmetric reduction

Table 2Textural properties of CuO/SiO₂ samples prepared by different precipitation agents.

Sample	Content (wt%) ^a		Crystallite size (nm) ^b		BET (m ² /g) ^c	D _{pore} (nm) ^c	Cu dispersion (%) ^d	S _{Cu} ^e (m ² /g Cu)	d _{Cu} ^f (nm)
	Cu	Na	CuO	Cu ⁰ used					
PGO-NaOH	26.7	0.07	5.4	10.2	186.1	13.0	19.6	138.3	5.1
PGO-Na ₂ CO ₃	26.1	0.07	B.D.	9.7	345.1	6.7	26.5	187.0	3.8
PGO-NH ₄ HCO ₃	24.4	B.D.	B.D.	26.4	382.6	8.0	29.9	210.9	3.3
PGO-NH ₄ OH	25.0	B.D.	29.3	40.2	112.5	9.4	14.7	103.7	6.8

^a Obtained from atomic absorption spectrometry (AAS) analysis. B.D. = below detection.^b Calculated from the Scherrer equation.^c BET method.^d Cu dispersion obtained from dissociative N₂O adsorption.^e Cu surface area measured by dissociative N₂O adsorption.^f Mean Cu particle size calculated from dissociative N₂O adsorption.**Table 3**XPS analysis of CuO/SiO₂ samples prepared by different precipitation agents.

Sample	Cu2p _{3/2} (eV)	FWHM of Cu2p _{3/2} (eV)	Cu/Si at		Assignment
			Bulk	Surface	
PGO-NaOH	935.6	4.1	0.349	0.405	CuO, Cu ₂ Si ₂ O ₅ (OH) ₂
PGO-NH ₄ OH	935.3	4.5	0.334	0.133	CuO, Cu ₂ Si ₂ O ₅ (OH) ₂
PGO-Na ₂ CO ₃	936.2	3.2	0.304	1.213	Cu ₂ Si ₂ O ₅ (OH) ₂
PGO-NH ₄ HCO ₃	936.3	2.7	0.314	1.096	Cu ₂ Si ₂ O ₅ (OH) ₂

peak centered around 534 K is most likely contributed by the one-step reduction of low interacted copper oxide (CuO–Cu⁰) and the partial reduction of highly dispersed and surface interacted copper species (Cu²⁺–Cu⁺).

Fig. 5 shows the TEM images of the calcined CuO/SiO₂ samples prepared with different precipitation agents. Both CuO nanowires and dispersed CuO particles were observed in PGO-NaOH (Fig. 5a), which is in line with our previous findings [46]. In calcined PGO-NH₄OH sample (Fig. 5b), randomly oriented filandrous species, which can be assigned to copper phyllosilicate according to the literature [43] and the above characterizations, along with a few large sheet like particles assignable to CuO were observed. The observation of large CuO particles in calcined PGO-NH₄OH sample is in line with XRD characterization. For calcined PGO-Na₂CO₃ and PGO-NH₄HCO₃ mainly randomly oriented filandrous copper phyllosilicate were seen (Fig. 5c,d). The highly diffusive ring pattern in the select area electron diffraction (SAED) of these two samples reveals an amorphous structure.

Table 4 shows the catalytic activities and selectivities of the Cu/SiO₂ catalysts prepared by PG method using different precipitants. As can be seen, PG-NaOH presented the highest initial activity. After 12 h reaction at 453 K and 9.0 MPa reaction pressure, a high conversion of 45.7% was obtained. Unexpectedly, the PG-NH₄HCO₃ catalyst with the highest Cu surface area (Table 2) showed a much lower conversion of 33.8%. The PG-Na₂CO₃ exhibited a moderate conversion of 36.8% and the PG-NH₄OH showed

the lowest conversion of 9.7%. The serious aggregation of Cu would be account for the inferior activities of the PG-NH₄HCO₃ and PG-NH₄OH catalysts, as their Cu⁰ crystallite sizes after reaction significantly sintered to 26.4 and 40.2 nm (Table 2), respectively. In addition, the serious leaching of active Cu species for PG-NH₄HCO₃ and PG-NH₄OH catalysts (>10 µg/g, Table 4), probably due to the presence of residual NH₄⁺ in these catalysts [33,37]. On the contrary, the residual Na in the PG-NaOH and PG-Na₂CO₃ may inhibit the sintering and leaching of Cu and thus contribute to the high reactivity of the catalysts [33,52]. Note that although the used PG-Na₂CO₃ presented essentially the same Cu crystallite size as the used PG-NaOH (9.7 vs. 10.2 nm), the former catalyst exhibited a lower activity than the latter. Previous studies reveal that glycerol hydrogenolysis reaction is likely a structure-sensitive reaction [28,33]. The rather small Cu particle size in the prereduced PG-Na₂CO₃ catalyst (< 4 nm, Table 2) might not facilitate for the conversion of glycerol, thus resulted in an inferior activity than PG-NaOH catalyst, whose initial Cu particle size is a bit larger (5.1 nm).

The product selectivities of the Cu/SiO₂ catalysts were also affected by the precipitation agent. The selectivities to 1,2-PDO for PG-NH₄HCO₃ and PG-NH₄OH were as high as 98.4 and 98.1%, respectively, which were around 3% higher than those for PG-NaOH and PG-Na₂CO₃ (both 95.3%). Inversely, the selectivities to EG were 2–2.5% higher for PG-NaOH and PG-Na₂CO₃ than for PG-NH₄HCO₃ and PG-NH₄OH. Such differences in product selectivities for the

Table 4Effect of precipitants on the catalytic performances of Cu/SiO₂ catalysts prepared by PG method.^a

Catalyst	Conversion (%)	Selectivity (%)			Leaching of Cu ²⁺ (µg/g)
		1,2-PDO	EG	Others ^b	
PG-NaOH	45.7	95.3	3.0	1.7	2.6
PG-NaOH ^c	38.4	96.0	2.6	1.4	2.2
PG-Na ₂ CO ₃	36.8	95.3	3.1	1.6	3.9
PG-Na ₂ CO ₃ ^c	25.8	96.2	2.3	1.5	2.5
PG-NH ₄ HCO ₃	33.8	98.4	0.7	0.9	11.2
PG-NH ₄ HCO ₃ ^c	9.7	99.0	0.3	0.7	10.9
PG-NH ₄ OH	5.3	98.1	0.6	1.3	14.3

^a Reaction conditions: 4 g reduced catalyst, 80 g 80 wt% glycerol aqueous solution, 453 K, total pressure 9.0 MPa, 12 h.^b Others: mainly methanol, ethanol and propanols.^c The catalyst reused for the second time.

Table 5

Composition, BET surface areas and crystallite sizes of the CuO-REO_x/SiO₂ samples calcined at 723 and 1023 K.

Sample	Composition RE/Cu/Si	S _{BET} ^a (m ² /g)	Crystallite size ^b (nm)	Sample	S _{BET} ^a (m ² /g)	Crystallite size ^b (nm)
Cu-0-723	0/1.0/3.0	180	5.6	Cu-0-1023	26	24.9
Cu-Y-723	0.083/1.0/3.0	151	5.6	Cu-Y-1023	95	7.7
Cu-La-723	0.095/1.0/3.0	144	5.8	Cu-La-1023	87	7.9
Cu-Ce-723	0.088/1.0/3.0	162	6.0	Cu-Ce-1023	38	20.7
Cu-Pr-723	0.089/1.0/3.0	150	5.7	Cu-Pr-1023	48	15.5
Cu-Sm-723	0.095/1.0/3.0	144	6.0	Cu-Sm-1023	50	13.7

^a BET method.

^b CuO crystallite size calculated from the Scherrer equation.

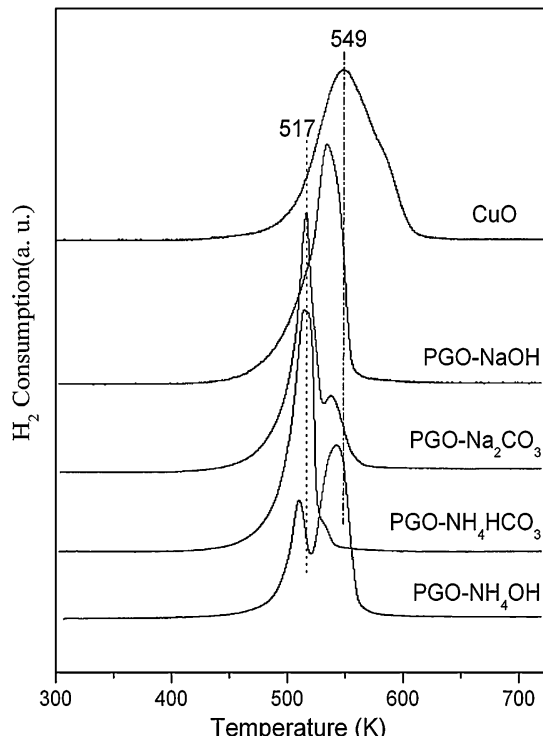


Fig. 4. TPR profiles of the calcined CuO/SiO₂ samples prepared by different precipitation agents: PGO-NH₄OH, PGO-NH₄HCO₃, PGO-Na₂CO₃, PGO-NaOH and the reference of bulk CuO.

Na-free PG-NH₄HCO₃ and PG-NH₄OH catalysts and the Na-containing PG-NaOH and PG-Na₂CO₃ catalysts indicate that it was the residual Na in Cu/SiO₂ catalyst mainly resulted in the formation of EG, which is in good agreement with previous detailed study on the effect of Na on the catalytic performance of Cu/SiO₂ catalyst [33].

To study the recycle ability as well as the deactivation behavior of the catalysts, we also carried out the recycle experiments of PG-NaOH, PG-Na₂CO₃ and PG-NH₄HCO₃. After reaction, the freshly used catalysts were filtrated and recharged into the autoclave together with the fresh reactant to perform the next run. As can be seen from Table 4, the reactivity of all the three catalysts in terms of conversion decreased to some extent after recycle, while their selectivity to 1,2-PDO slightly increased. Serious loss of activity, decreased by ~71%, was observed on the reused PG-NH₄HCO₃, while only moderate decrease of activity, decreased by 16 and 30% was seen for the PG-NaOH and PG-Na₂CO₃ catalysts after recycle, respectively. The profound sintering of Cu particles and serious leaching of active Cu would be account for the significant deactivation of PG-NH₄HCO₃. Besides the sintering and leaching of Cu, the presence of strongly adsorbed species (reactant and/or products) on the catalysts surface may also resulted the deactivation of the

catalysts [28]. In comparison with PG-Na₂CO₃, the higher recycle stability for PG-NaOH would be ascribed to its more even dispersion of Cu species, as revealed by XPS analysis (Table 3), which increased the reaction stability of the catalyst.

3.2. Effect of rare earth additives on the structure and catalytic performance of Cu/SiO₂ catalysts

From the above studying one knows that the reaction stability of the single-component Cu/SiO₂ catalysts, even for the most stable PG-NaOH catalyst, is still unsatisfactory. To improve the stability of the Cu/SiO₂ catalyst, a variety of rare earth (RE) elements including La, Ce, Y, Pr and Sm were incorporated into the Cu/SiO₂ catalyst prepared by PG method using NaOH as precipitant. Fig. 6 shows the XRD patterns of CuO-REO_x/SiO₂ samples calcined at 723 K (A) and 1023 K (B). In comparison with Cu-0-723, no big differences were seen after the incorporation of Y, La, Pr and Sm, while additional diffractions assignable to CeO₂ were seen for Cu-Ce-723. After calcination at a relatively high temperature of 1023 K, the diffractions of CuO for all samples intensified, especially noticeable for Cu-0-1023 (Fig. 6B). Compared with Cu-0-1023, the lower and broader diffractions of CuO for the RE-incorporated samples refer a lower sintering of CuO particles, especially for Cu-Y-1023 and Cu-La-1023. Except for Cu-Ce-1023, no diffractions related to REO_x were seen for the Y, La, Pr and Sm incorporated samples, even after calcined at 1023 K, probably due to the low contents and the much high dispersion of these REO_x in the samples.

Table 5 shows the textural properties of the CuO/SiO₂ samples prepared by PG method with and without incorporation of RE calcined at two different temperatures of 723 and 1023 K. No big differences in crystallite sizes were observed between the samples without and with the incorporation of RE after calcination at 723 K. While a slight decrease in surface area of all the RE-incorporated samples was seen as compared to the mother CuO/SiO₂ sample, probably due to the coverage of the sample surface with REO_x particles and blocking of some pores by REO_x particles. After calcination at a much high temperature of 1023 K, the CuO crystallite size for the non-RE incorporated Cu/SiO₂ sample remarkably increased to 24.9 nm, while the sizes for all RE-doped samples were below 21 nm, especially noticeable for Y and La incorporated samples, which are 7.7 and 7.9 nm, respectively (Table 5). These results indicate that the incorporated REO_x particles, which insert between CuO particles and/or cover on CuO particles (partial or full), could prevent the sintering of Cu particles. The BET surface areas of all the RE-doped samples were larger than that of the none-RE incorporated CuO/SiO₂ sample (decreased to just 26 m²/g) with the surface areas of Y and La incorporated samples much larger, which are around 3.5 times that of the mother sample, showing that the incorporation of RE could remarkably enhance the thermal resistance of the samples, probably by inhibiting the loss of the support surface area. The above findings suggest that the incorporation of RE to CuO/SiO₂ sample, especially Y and La, could inhibit the sintering of the sample and thus maintain high thermal stability of the samples.

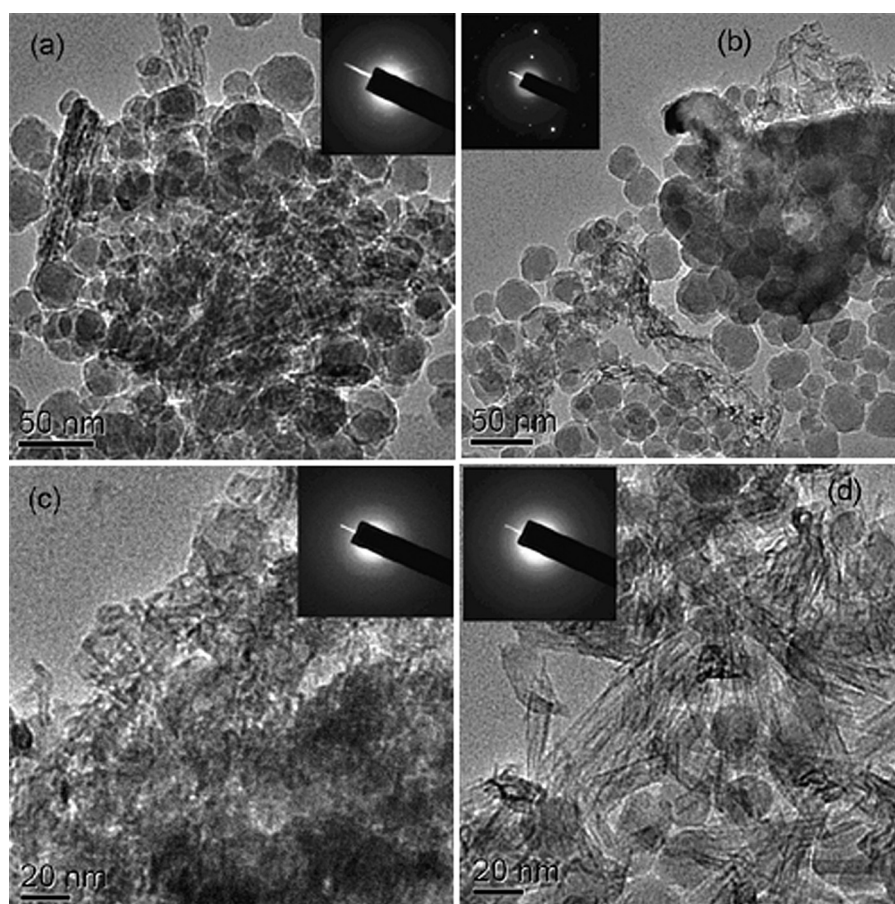


Fig. 5. TEM images of samples prepared by different precipitation agents: (a) PGO-NaOH, (b) PGO-NH₄OH, (c) PGO-Na₂CO₃ and (d) PGO-NH₄HCO₃.

Table 6 shows the catalytic activity test of the Cu/SiO₂ catalysts with and without the incorporation of REO_x calcined at 723 and 1023 K in glycerol hydrogenolysis in non-continuous autoclave. As can be seen, for the catalysts calcined at 723 K, the undoped Cu/SiO₂ showed a high conversion of 73.3% after reaction at 473 K for 10 h, while all the RE-incorporated catalysts presented lower conversions, lowered by 10–29%. The decrease of activity for the RE-incorporated catalysts would be resulted by partially covering of the active sites by REO_x particles. However, after calcination at 1023 K, the conversion of the undoped Cu/SiO₂ catalyst sharply decreased to 24.7% (decreased by 66%), while only slight decrease of conversions (17–19%) were seen for the Y, La, Ce, and Sm

incorporated catalysts. The conversion of Pr-incorporated catalyst even increased from 44.3 to 52.1% after calcined at 1023 K. The conversions of all the RE-incorporated catalysts calcined at 1023 K were around 2 times higher than that of undoped Cu/SiO₂, showing that the incorporation of RE to Cu/SiO₂ catalyst could greatly promote the reaction stability of the catalysts, even after treating under serious conditions. The promotional effects of RE may be originated from the following aspects: first the incorporation of RE prevented the sintering of Cu and thus maintained the high dispersion of the active Cu, second the electronic transfer from RE would decrease the electron density of active Cu and stabilize the active sites in their appropriate valence state [53], third the

Table 6

Catalytic activity and selectivity of glycerol hydrogenolysis over Cu-REO_x/SiO₂ catalysts calcined at 723 and 1023 K.^a

Catalyst	Conversion (%)	Selectivity (%)			Leaching of Cu ²⁺ ($\mu\text{g/g}$)
		1,2-PDO	EG	Others ^b	
Cu-0-723	73.3	92.2	7.1	0.7	6.9
Cu-Y-723	62.0	93.9	4.7	1.4	0.4
Cu-La-723	63.2	92.6	5.7	1.7	0.9
Cu-Ce-723	62.7	93.4	5.5	1.1	0.8
Cu-Pr-723	44.3	93.6	4.8	1.6	0.3
Cu-Sm-723	57.4	92.4	5.5	2.1	0.4
Cu-0-1023	24.7	94.5	4.6	0.9	N.D.
Cu-Y-1023	51.2	94.6	4.6	0.8	N.D.
Cu-La-1023	51.6	93.9	5.1	1.0	N.D.
Cu-Ce-1023	50.6	93.5	5.6	0.9	N.D.
Cu-Pr-1023	52.1	93.5	5.5	1.0	N.D.
Cu-Sm-1023	47.2	93.9	5.0	1.1	N.D.

^a Reaction condition: 1.0 g reduced catalyst, 20 g 80% glycerol aqueous solution, 473 K, 8 MPa H₂, 10 h. (N.D. = not determined).

^b Others: mainly methanol, ethanol and propanols.

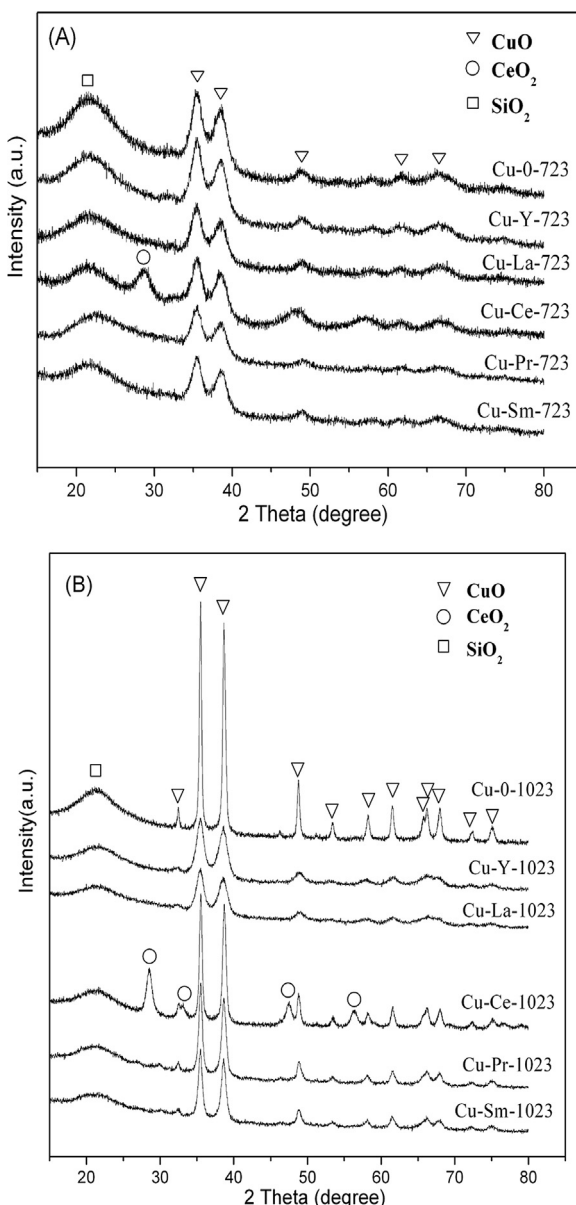


Fig. 6. XRD patterns of Cu-REO_x/SiO₂ samples calcined at 723 K (A) and 1023 K (B).

synergistic effect between RE-involved sites could increase the reaction activity [36,54]. In addition, the incorporation of RE could retard the leaching of active Cu, as which sharply declined from 6.9 µg/g for Cu/SiO₂ catalyst to below 0.9 µg/g for the RE-doped catalysts (Table 6), which would also benefit for the reaction stability of the RE-doped catalysts. It should be noted that the selectivity to 1,2-PDO maintained at around 92.2–94.6%, seems not to be affected much by the incorporation of RE as well as the pretreatment temperatures.

To date, the high deactivation and inadequate lifetime of Cu-based catalysts remain significant problems that hinder the practical industrialization of glycerol hydrogenolysis to 1,2-PDO. Since the incorporation of La could greatly improve the structure stability of the Cu/SiO₂ catalyst, and also exhibited a higher glycerol reactivity than other Re-doped catalysts, the long-term catalytic performances of the La-doped Cu/SiO₂ catalyst and unmodified Cu/SiO₂ catalysts were compared in the liquid phase hydrogenolysis of glycerol at 453 K and 6 MPa reaction pressure (Fig. 7). The Cu-La-723 catalyst showed a lower initial conversion of 78%, but retained a steady conversion of ~70% after a 600 h time-on stream

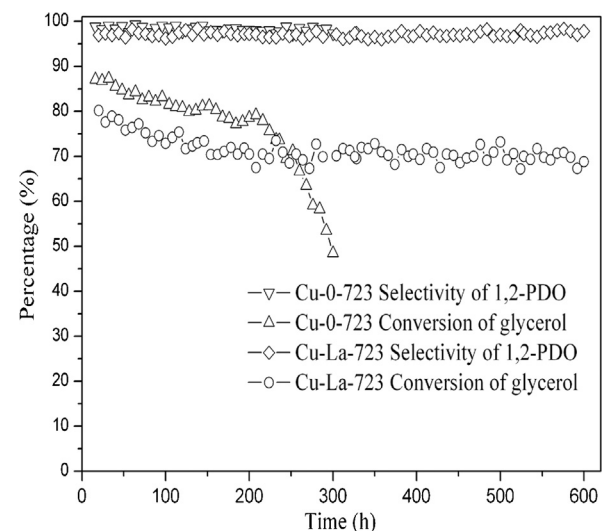


Fig. 7. Time on-stream behavior of Cu-0-723 and Cu-La-723 catalysts. Reaction conditions: WHSV of 0.25 h⁻¹, glycerol to hydrogen mole ratio 1:23, pressure 6.0 MPa, 453 K.

reaction. Although the Cu-0-723 catalyst exhibited a higher initial conversion of 87%, it rapidly deactivated after around 220 h reaction. Both catalysts maintained high 1,2-PDO selectivities of around 97–98% in the continuous flow reaction conditions. The remarkable increase of long-term stability of the Cu-La-723 clearly confirmed the promotion effect of RE on the reaction stability of the Cu/SiO₂ catalyst. The decrease of initial activity over Cu-La-723 catalyst in continuous fixed-bed flow reactor is in agreement with the results obtained in non-continuous autoclave reaction. Although the conversion of the La-doped Cu/SiO₂ catalyst needs further improvement, which can be achieved by increasing reaction temperature or decreasing the WHSV as reported previously [21,27], its long-term stability and high selectivity toward 1,2-PDO are very attractive, especially from the practical aspects for industrial applications.

4. Conclusions

The effects of the precipitation agents (NaOH, Na₂CO₃, NH₄OH and NH₄HCO₃) and rare earth additives (La, Ce, Y, Pr and Sm) on the structure and catalytic performance in glycerol hydrogenolysis of the Cu/SiO₂ catalysts prepared by precipitation-gel method have been studied. Characterization results showed that the surface structure and composition of the Cu/SiO₂ catalysts differ greatly by the precipitation agents applied. Due to a more even dispersion of Cu particles, a higher resistant to sintering and leaching of active Cu, the catalyst prepared by NaOH exhibited the highest activity and stability in glycerol hydrogenolysis than those by other precipitants, however, a slight decrease of selectivity to 1,2-PDO due to the presence of residual Na⁺ was seen. The incorporation of rare earth additives, especially Y and La, to Cu/SiO₂ catalyst could obviously inhibit the sintering and leaching of Cu, and thus maintain high thermal stability and long-term reaction stability of the catalysts. These findings shed light on the design of more efficient and stable catalysts for the industrial application of glycerol hydrogenolysis to 1,2-PDO.

Acknowledgements

The authors gratefully acknowledge the financial support from the National Natural Science Foundation of China (Grant Nos. 21133011, 21203221) and Science and Technology Support Program of Gansu Province, China (Grant No. 1304FKCA113).

References

- [1] A.J. Ragauskas, C.K. Williams, B.H. Davison, G. Britovsek, J. Cairney, C.A. Eckert, W.J. Frederick Jr., J.P. Hallett, D.J. Leak, C.L. Liotta, J.R. Mielenz, R. Murphy, R. Templer, T.Tschaplinski, *Science* 311 (2006) 484–489.
- [2] A. Corma, S. Iborra, A. Velty, *Chem. Rev.* 107 (2007) 2411–2502.
- [3] D.M. Alonso, J.Q. Bond, J.A. Dumesic, *Green Chem.* 12 (2010) 1493–1513.
- [4] J.C. Serrano-Ruiz, R. Luque, A. Sepúlveda-Escribano, *Chem. Soc. Rev.* 40 (2011) 5266–5281.
- [5] A.M. Ruppert, K. Weinberg, R. Palkovits, *Angew. Chem. Int. Ed.* 51 (2012) 2564–2601.
- [6] J. ten Dam, U. Hanefeld, *ChemSusChem* 4 (2011) 1017–1034.
- [7] C.H. Zhou, H. Zhao, D.S. Tong, L.M. Wu, W.H. Yu, *Catal. Rev. Sci. Eng.* 55 (2013) 369–453.
- [8] T. Miyazawa, Y. Kusunoki, K. Kunimori, K. Tomishige, *J. Catal.* 240 (2006) 213–221.
- [9] E.P. Maris, R.J. Davis, *J. Catal.* 249 (2007) 328–337.
- [10] I. Furukado, T. Miyazawa, S. Koso, A. Shima, K. Kunimori, K. Tomishige, *Green Chem.* 9 (2007) 582–588.
- [11] I. Gandarias, P.L. Arias, J. Requies, M.B. Güemez, J.L.G. Fierro, *Appl. Catal. B* 97 (2010) 248–256.
- [12] S. Wang, K. Yin, Y. Zhang, H. Liu, *ACS Catal.* 3 (2013) 2112–2121.
- [13] M.A. Dasari, P.-P. Kiatsimkul, W.R. Sutterlin, G.J. Suppes, *Appl. Catal. A* 281 (2005) 225–231.
- [14] Z. Huang, F. Cui, H. Kang, J. Chen, X. Zhang, C. Xia, *Chem. Mater.* 20 (2008) 5090–5099.
- [15] L. Guo, J. Zhou, J. Mao, X. Guo, S. Zhang, *Appl. Catal. A* 367 (2009) 93–98.
- [16] S. Wang, Y. Zhang, H. Liu, *Chem. Asian J.* 5 (2010) 1100–1111.
- [17] W. Yu, J. Zhao, H. Ma, H. Miao, Q. Song, J. Xu, *Appl. Catal. A* 383 (2010) 73–78.
- [18] Q. Liu, X. Guo, Y. Li, W. Shen, *J. Phys. Chem. C* 113 (2009) 3436–3441.
- [19] S. Xia, R. Nie, X. Lu, L. Wang, P. Chen, Z. Hou, *J. Catal.* 296 (2012) 1–11.
- [20] F. Vila, M. López Granados, M. Ojeda, J.L.G. Fierro, R. Mariscal, *Catal. Today* 187 (2012) 122–128.
- [21] S. Zhu, X. Gao, Y. Zhu, Y. Zhu, H. Zheng, Y. Li, *J. Catal.* 303 (2013) 70–79.
- [22] A. Bienholz, F. Schwab, P. Claus, *Green Chem.* 12 (2010) 290–295.
- [23] J. Zhou, L. Guo, X. Guo, J. Mao, S. Zhang, *Green Chem.* 12 (2010) 1835–1843.
- [24] D. Durán-Martín, M. Ojeda, M.L. Granados, J.L.G. Fierro, R. Mariscal, *Catal. Today* 210 (2013) 98–105.
- [25] Z. Yuan, J. Wang, L. Wang, W. Xie, P. Chen, Z. Hou, X. Zheng, *Bioresour. Technol.* 101 (2010) 7088–7092.
- [26] Z. Xiao, J. Xiu, X. Wang, B. Zhang, C.T. Williams, D. Su, C. Liang, *Catal. Sci. Technol.* 3 (2013) 1108–1115.
- [27] L. Huang, Y.L. Zhu, H.Y. Zheng, Y.W. Li, Z.Y. Zeng, *J. Chem. Technol. Biotechnol.* 83 (2008) 1670–1675.
- [28] E.S. Vasiliadou, T.M. Eggenhuisen, P. Munnik, P.E. de Jongh, K.P. de Jong, A.A. Lemonidou, *Appl. Catal. B* 145 (2014) 108–119.
- [29] A. Bienholz, R. Blume, A. Knop-Gericke, F. Girsdes, M. Behrens, P. Claus, *J. Phys. Chem. C* 115 (2010) 999–1005.
- [30] S.L. Hao, W.C. Peng, N. Zhao, F.K. Xiao, W. Wei, Y.H. Sun, *J. Chem. Technol. Biotechnol.* 85 (2010) 1499–1503.
- [31] N.D. Kim, S. Oh, J.B. Joo, K.S. Jung, J. Yi, *Top. Catal.* 53 (2010) 517–522.
- [32] C.V. Rode, A.A. Ghalwadkar, R.B. Mane, A.M. Hengne, S.T. Jadkar, N.S. Biradar, *Org. Process Res. Dev.* 14 (2010) 1385–1392.
- [33] Z. Huang, F. Cui, H. Kang, J. Chen, C. Xia, *Appl. Catal. A* 366 (2009) 288–298.
- [34] E.S. Vasiliadou, A.A. Lemonidou, *Appl. Catal. A* 396 (2011) 177–185.
- [35] Z. Huang, F. Cui, J. Xue, J. Zuo, J. Chen, C. Xia, *Catal. Today* 183 (2012) 42–51.
- [36] J. Zuo, Z. Huang, F. Cui, J. Chen, C. Xia, *Chin. J. Mol. Catal.* 24 (2010) 195–201.
- [37] X.F. Dong, H.B. Zou, W.M. Lin, *Int. J. Hydrogen Energy* 31 (2006) 2337–2344.
- [38] C.J.G. Van Der Grift, A.F.H. Wielers, B.P.J. Joghi, J. Van Beijnum, M. De Boer, M. Verslujs-Helder, J.W. Geus, *J. Catal.* 131 (1991) 178–189.
- [39] T. Touponce, M. Kermarec, J.-F. Lambert, C. Louis, *J. Phys. Chem. B* 106 (2002) 2277–2286.
- [40] G. Díaz, R. Pérez-Hernández, A. Gómez-Cortés, M. Benassa, R. Mariscal, J.L.G. Fierro, *J. Catal.* 187 (1999) 1–14.
- [41] Z. Wang, Q. Liu, J. Yu, T. Wu, G. Wang, *Appl. Catal. A* 239 (2003) 87–94.
- [42] T.M. Yurieva, G.N. Kustova, T.P. Minyukova, E.K. Poels, A. Bliek, M.P. Demeshkina, L.M. Plyasova, T.A. Krieger, V.I. Zaikovskii, *Mater. Res. Innovat.* 5 (2001) 3–11.
- [43] L.F. Chen, P.J. Guo, M.H. Qiao, S.R. Yan, H.X. Li, W. Shen, H.L. Xu, K.N. Fan, *J. Catal.* 257 (2008) 172–180.
- [44] C.J.G. Van Der Grift, P.A. Elberse, A. Mulder, J.W. Geus, *Appl. Catal. A* 59 (1990) 275–289.
- [45] K.V.R. Chary, K.K. Seela, G.V. Sagar, B. Sreedhar, *J. Phys. Chem. B* 108 (2004) 658–663.
- [46] Z. Huang, F. Cui, J. Xue, J. Zuo, J. Chen, C. Xia, *J. Phys. Chem. C* 114 (2010) 16104–16113.
- [47] X.C. Zheng, S.P. Wang, S.R. Wang, S.M. Zhang, W.P. Huang, S.H. Wu, *Mater. Sci. Eng. C* 25 (2005) 516–520.
- [48] M.A. Kohler, H.E. Curry-Hyde, A.E. Hughes, B.A. Sexton, N.W. Cant, *J. Catal.* 108 (1987) 323–333.
- [49] A.J. Marchi, J.L.G. Fierro, J. Santamaría, A. Monzón, *Appl. Catal. A* 142 (1996) 375–386.
- [50] E.D. Guerreiro, O.F. Gorri, G. Larsen, L.A. Arrúa, *Appl. Catal. A* 204 (2000) 33–48.
- [51] F.W. Chang, W.Y. Kuo, K.C. Lee, *Appl. Catal. A* 246 (2003) 253–264.
- [52] J. Llorca, N.s. Homs, J. Sales, J.-L.G. Fierro, P. Ramírez de la Piscina, *J. Catal.* 222 (2004) 470–480.
- [53] R. Kam, C. Selomulya, R. Amal, J. Scott, *J. Catal.* 273 (2010) 73–81.
- [54] X. Zheng, X. Zhang, X. Wang, S. Wu, *Appl. Catal. A* 295 (2005) 142–149.